Stochastic evaluation of annual micropollutant loads and their uncertainties in separate storm sewers

Ali Hannouche, Ghassan Chebbo, Claude Joannis, Johnny Gasperi, Marie-Christine Gromaire, Régis Moilleron, Sylvie Barraud, Véronique Ruban

Stochastic evaluation of annual micropollutant loads and their uncertainties in separate storm sewers

Hannouche, A.[1,*]; Chebbo, G.[1, 2], Joannis, C.[3], Gasperi J.[1]; Gromaire M.C.[1], Moilleron R.[(1)], Barraud S.[3], Ruban V.[3]

[1] Université Paris-Est, LEESU (UMR-MA-102), UPEC, UPEMLV, ENPC, Agro ParisTech, 6 et 8 avenue Blaise Pascal - Cité Descartes, 77455 Champs-sur-Marne Cedex 2, France
[2] Faculty of Engineering III, Lebanese University, Hadath – Lebanon
[3] LUNAM, IFSTTAR – LEE, Département Géotechnique Eau, Risques naturels et Sciences de la terre – Laboratoire Eau et Environnement- route de Bouaye CS4 – 44344 Bouguenais cedex
[4] Université de Lyon, INSA Lyon, Université Lyon1, DEEP, 34 avenue des Arts, 69621 Villeurbanne cedex, France
Corresponding author: * ali.hannouche@leesu.enpc.fr; +33(0) 1.64.15.39.50; +33(0) 1.64.15.37.64

Abstract:
This article describes a stochastic method to calculate the annual pollutant loads and its application over several years at the outlet of three catchments drained by separate storm sewers. A stochastic methodology using Monte Carlo simulations is proposed for assessing annual pollutant load, as well as the associated uncertainties, from a few event sampling campaigns and/or continuous turbidity measurements (representative of the Total Suspended Solids concentration (TSS)). Indeed, in the latter case, the proposed method takes into account the correlation between pollutants and TSS. The developed method was applied to data acquired within the French research project "INOGEV" (Innovations for a sustainable management of urban water) at the outlet of three urban catchments drained by separate storm sewers. Ten or so event sampling campaigns for a large range of pollutants (46 pollutants and 2 conventional water quality parameters: TSS and total organic carbon (TOC)) are combined with hundreds of rainfall events for which, at least one among three continuously monitored parameters (rainfall intensity, flow rate and turbidity) is available.
Results obtained for the three catchments show that the annual pollutant loads can be estimated with uncertainties ranging from 10% to 60%, and the added value of turbidity monitoring for lowering the uncertainty is demonstrated. A low inter-annual and inter-site variability of pollutant loads, for many of studied pollutants, is observed with respect to the estimated uncertainties, and can be explained mainly by annual precipitation.

Keywords: Stormwater; database; pollutant; annual load; turbidity; TSS; uncertainties; variability.

INTRODUCTION

In the case of separate storm sewers, runoff is usually discharged directly into the natural environment without any treatment. These discharges constitute a continuous and significant vector of pollutants towards receiving waters (Becouze-Lareure et al. 2011, Clark et al. 2007, Weiss et al. 2008, Zgheib et al. 2012). The reduction of these discharges is a major issue of the EU Water Framework Directive (WFD) (2013/39/EU) to achieve the "good ecological status" for all of Europe's surface waters and groundwater. This challenge requires accurate knowledge of pollutant loads discharged by separate sewer. Beyond the conventional water quality parameters (Total Suspended Solids (TSS); Chemical Oxygen Demand (COD); etc.) extensively studied over several decades, monitoring of priority and/or emerging substances has become an important issue in Europe to meet the requirements of the WFD (Sebastian et al. 2011). Due to financial costs, operational and technical issues, the assessment of pollutant loads is constrained by a lack of suitable measuring devices. Monitoring is frequently carried out by taking samples for subsequent analysis in the laboratory. Analytical methods are standardized but still pollutant dependant. Yet, the sampling process has some major drawbacks, among which the limited number of samples which can practically be handled due to random occurrence of rain events, frequent maintenance, etc. Indeed, monitoring programs prove to be very costly and require considerable staff time. Only a limited number of campaigns (generally less than 5) are thus carried out during a given year (Gromaire et al. 2007) for operational purposes, and data are usually pooled to derive an Annual (or Site-specific) discharge-weighted (or arithmetic) Mean Concentration SMC, whose value is then multiplied by the total runoff volume of the considered period to assess pollutant loads. This method induces large uncertainty values (Mourad et al. 2005).

Besides these considerations TSS have been revealed as the predominant pollutant vector in sewer systems (Ashley et al. 2005, Zgheib et al. 2012). In fact, for some pollutants such as PAH, PCB and metals, TSS is a significant vector, while isn't for other pollutants such as Octylphenol OP, TSS is not the significant vector (Zgheib et al. 2012).

Continuous turbidity measurements can now provide recordings which are representative of the TSS concentration. Actually, turbidity can be translated into TSS concentration by using an average TSS-Turbidity relationship at different time-scales (Hannouche et al. 2011, Lacour et al. 2009, Langeveld et al. 2005, Metadier and Bertrand-Krajewski 2012). TSS concentration time-series are thus made available. The use of continuous measurement data (rain intensity, flow rate, turbidity), in addition to a limited number of laboratory analysis by sampling, therefore enables a more accurate assessment of the annual micropollutants flux.

In this context, the "INOGEV" project (*Innovations for a sustainable management of urban water*) was launched in early 2010 by the national network of French observatories in urban hydrology "SOERE URBIS" (*A long-term Observation System for research and Experimentation on urban environment*) combining the works of "OPUR" in Paris (*Observatory of Urban Pollutants in Île-de- France/Paris region, since 1994*), "OTHU" in Lyon (*Field Observatory for Urban Water Management in Lyon-France, since 1999*) and "ONEVU" in Nantes (*Observatory of urban environments of Nantes- France, since 2006*). This project aimed at improving the knowledge and control of the contamination of urban stormwater in a multidisciplinary approach as regards scientific research, operational practices and social understanding. By harmonizing scientific approaches and monitoring methodologies (pollutants, sampling, analytical methods and results interpretation) at the scale of three urban districts featuring distinct land use patterns and contexts, a new extended

French dataset has been built for a large range of pollutants at the event scale (Gasperi et al. 2014). In addition, the observatories had formerly provided some statistically representative databases for water flow rate and turbidity measurements for several years at the outlet of two of the three studied catchments.

In this paper, a combined approach was adopted coupling the new dataset of pollutant concentrations and available recordings of hydrological and water quality parameters (rainfall intensity, flow rate, turbidity), to assess annual pollutant loads as well as the associated uncertainties. First the databases used are briefly presented. Then, the methodology developed to assess the annual loads and their uncertainty for a given pollutant including the underlying hypotheses is described. Results obtained are then discussed and compared between the three sites.

EXPERIMENTAL DATA

Sites description

Three experimental sites drained by a separate sewer systems (*Sucy* in Île-De-France/Paris region, *Chassieu* in Lyon and *Pin Sec* in Nantes) were considered. *Table 1* summarizes the main characteristics and the available databases at the three sites. Their areas range from 30 to 228 ha and their runoff coefficients (*RC*) vary between 22 (*Sucy*) to 30% (*Chassieu*). *Chassieu* is an industrial catchment while other catchments are residential with mostly small private houses and limited commercial and professional activity (small shops and services) at *Sucy* catchment, and mainly collective buildings and private houses at *Pin Sec* catchment. On the whole, most of buildings and houses were built between the years1970 and 1980.

Table 1: Sites and databases available

Sites	Location	Area	RC[1]	Land use	Slope	Available data
Sucy	Paris, South-East	228 ha	0.22	Residential	0.2%	- Continuous rainfall intensity, flow and turbidity measurements (Time step=2 min; 2011-2012): 121/220 rain events [(2, a)]; - Sampled rainfall events [(3)] : 24 (7-10 [(4)])
Chassieu	Lyon, East	185 ha	0.30	Industrial	0.4%	- Continuous rainfall intensity, flow and turbidity measurements (Time step=2 min; 2004-2008): 263/655 rain events [(2, a)]; - Sampled rainfall events [(3)]: 7 (2-5 [(4)])
Pin Sec	Nantes, North-East	30 ha	0.26	Residential and collective housing	1.0%	- Continuous rain intensity and flow measurements (Time step=5 min; 2011-2012): 198/214 rain events (2, b); - Sampled rainfall events (3): 18 (7-15 (4))

(1) RC = runoff coefficient (see Precipitation – volume model (Model M1) for more information), (2) number of rainfall events with: (a), valid flow and turbidity measurements compared to all identified rain events, (b) valid flow measurements compared to all identified rain events (no turbidity measurement at Pin Sec site); (3) Number of rainfall events sampled at each site with measurements of global parameters; (4) Number of rain events analyzed for each group of micropollutants.

Available monitoring data

Sampled rainfall events and measured pollutants

Depending on the site under consideration, between 7 and 24 rainfall events were sampled from July 2011 to May 2013 with automatic samplers controlled by a flow-meter to obtain flow proportional event mean concentrations (EMC). The sampling equipment and field blank procedures were harmonized between observatories and described in (Gasperi et al. 2014).

The main characteristics of these events such as precipitation depth (H in *mm*), mean and max intensity in 5 min (I_{mean} and I_{max} in $mm.h^{-1}$) and preceding dry weather period (PDWP in days) are given in *Table 6* in supplementary materials section. On the whole, these rainfall events feature relatively low rainfall intensities, with no extreme rainfall amounts collected.

Conventional water quality parameters, such as TSS and total dissolved and particulate organic carbon (TOC, DOC and POC), were analyzed for each rain event sampled. A total of 46 micropollutants were monitored for 2 to 15 rainfall events, including 13 metals, 16 polycyclic aromatic hydrocarbons (PAH), 9 polybromodiphenylethers (PBDE), bisphenol A (BPA) and 7 alkylphenols (APnEOs). The full list of targeted molecules and the usual abbreviations are listed extensively in *Table 7* supplementary materials section.

Continuous measurements

All sites are equipped with monitoring stations for rainfall intensity, flow rate. Rainfall intensities at each catchment area were measured by tipping bucket rain gauges. Raw data were converted into 5 min time step time series. The flow rates are derived from both water level and flow velocity monitoring at the outlet of each catchment. Turbidity was monitored continuously at Sucy and Chassieu, with two redundant turbidity sensors at a 2 min time step:

- In *Sucy* site, 2 turbidimeters (Ponselle brand, TU-TRANS-NA) with attenuation at 880 nm and calibration using formazin (range=0-2000 FAU (Formazin Attenuation Unit)) are used. The sensors are installed in the storm sewer pipe, next to the point of flow measurement.
- In *Chassieu* site, 2 turbidimeters (one Endress-Hauser W CUS31 and one Dr Lange Solitax) with nephelometry at 860 nm and calibration using Formazin (range =0-4000 FNU (Formazin Nephelometry Unit)) are used. The turbidity is measured in an off-line monitoring flume installed in a shelter located above ground (Metadier and Bertrand-Krajewski 2012). Water is pumped from the sewer into the flume by a peristaltic pump at approximately 1 L/s and a suction velocity of approximately 1 m/s to avoid settling and particle segregation in the pumping tube.

Turbidity data were processed and validated by using redundancy in *Sucy* (Lacour et al. 2009) site or by using the method detailed in (Mourad and Bertrand-Kralewski 2002) in *Chassieu* site.

Storm events are identified using flow rate and rainfall intensity. The beginning of the event is given by the rise of the flow rate signal whereas the end of the event is given by the return to the dry weather base-flow attributed to groundwater infiltration. In a second step, the runoff events identified are compared to rainfall data to eliminate all hydrographs which correspond to a precipitation depth lower than *0.5 mm* (< Initial loss, see Precipitation – volume model (Model M1) for more information). During the years 2011 and 2012: i) 220 rain events have been identified for *Sucy* site including 121 rainfall events with valid flow and turbidity measurements, ii) and 214 rain events for *Pin Sec* site among which 198 events possess valid flow measurements). Over the period 2004–2008 in *Chassieu* site, the final validated database (flow and turbidity) contains 263 events among 655 identified rain events (*Table 1*). Indeed, data acquired at this site between 2011 and 2012 was not exploitable because of the failures of the peristaltic pump.

The main characteristics of these rainfall events are given in *Table 2*. The characteristics of these rainfall events are with the same magnitude as those sampled during the pollutant sampling campaigns.

Table 2: Main rainfall characteristics of the identified rain events on the three study sites (d_{10}-d_{50}-d_{90}).

	H (mm)(1)	Duration (h)	I_{mean} ($mm.h^{-1}$)	I_{max}($mm.h^{-1}$)(2)	PDWP (3)
Sucy (n=121)	1.4-5.0-12.7	1.0-4.7-13.0	0.6-1.3-2.7	2.4-4.8-21.6	0.22-1.29-5.12
Chassieu (n=263)	1.0-2.4-14.7	0.7-3.5-13.0	0.3-1.1-2.8	1.5-4.4-17.5	0.25-0.65-5.6
Pin Sec (n=198)	1.3-3.2-13.0	0.7-2.2-11.8	0.8-2.2-3.6	3.1-7.3-15.5	0.11-0.97-9.54

1) Precipitation depth; 2) I_{max} evaluated over 5-min intervals; 3) Preceding dry weather period, in days.

TSS-Turbidity correlation functions and uncertainties

Previous research demonstrated that linear or polynomial function can be used to estimate TSS concentration from turbidity (Hannouche et al. 2011, Metadier and Bertrand-Krajewski 2012).

For *Sucy*, the discharge–weighted event mean turbidity (EMT) was calculated from the continuous and validated turbidity measurements for 14 rainfall events among the 24 rainfall events sampled in *Sucy* site. The 14 pairs (EMT, TSS) obtained allowed us to build the TSS-turbidity linear function (*Figure 1 , (a); $TSS_{(mg/l)}=f(EMT_{(FAU)})=31.9+0.45EMT$,* (Equation 1)) at the event scale. For each rainfall event *j* for which there is a validated turbidity pollutograph (T_{ij}) (*i* is an index of the time step) and flow rate hydrograph (Q_{ij}), a discharge–weighted event mean turbidity is calculated $T_j \approx \frac{\sum_{i=1}^{n_j} T_{ji} \times Q_{ji} \times \Delta t_{ji}}{\sum_{i=1}^{n_j} Q_{ji} \times \Delta t_{ji}}$ (Equation 2) and then transformed into TSS event mass by applying the TSS-turbidity linear function established on this site. Finally, the residual error implied by this conversion is assessed by assuming that residual errors follow a normal distribution with same variance derived from residues observed for calibration data (Hannouche et al. 2011).

About sixty grab sample were taken in *Chassieu* site by (Metadier and Bertrand-Krajewski 2012) during wet weather conditions between 2002 and 2008 (we have no information on the number of sampled events). For each sample, 25 repeated turbidity measurements and triplicate TSS analysis according to usual standards methods are carried out, including assessment of uncertainties. These have allowed to build a second degree polynomial function ($TSS_{(mg/l)}$=12.9+0.7*$T_{(FNU)}$+7. 8e−4*$T^2_{(FNU)}$, (Equation 3)) by means of Williamson weighted least squares regression method accounting for uncertainties in both coordinates (TSS and turbidity) A detailed description of this method and uncertainty estimation are reported in (Metadier and Bertrand-Krajewski 2011). The obtained correlation function in *Chassieu* is given in *Figure 1 , (b)*.

Note that the difference in procedure for estimation of TSS concentration at both sites is due to the methods of turbidity measurements and to available TSS-Turbidity data on each site.

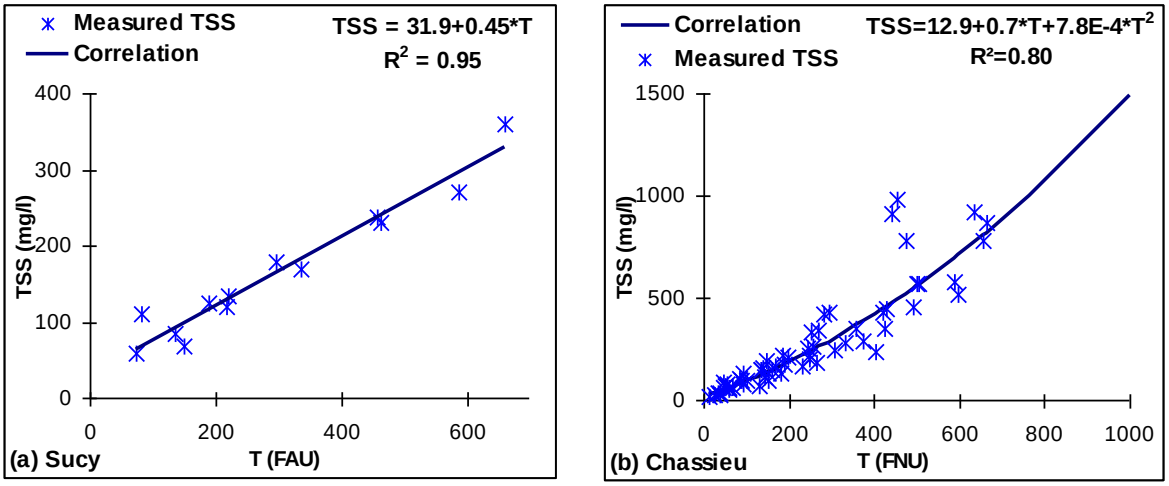

Figure 1: TSS-Turbidity correlation functions: (a) *Sucy* ; (b) *Chassieu*

The two correlation functions on both sites are different. This may be mainly due to measuring and calculation methods used at each site (attenuation in *Sucy* and nephelometry in *Chassieu*). Indeed, at the *Chassieu* site, this relationship was established by (Metadier and Bertrand-Krajewski 2011) for instantaneous samples with turbidity measured in nephelometry. While on the *Sucy* site, we calculated event mean turbidity for rain events (which are less variable than those of instantaneous turbidities), for which the event mean concentration and turbidity pollutograph are known. Moreover, although the y-intercept (measurement offset) at *Sucy* site is quite high (31.9 mg/l TSS at 0 FAU), its variability at 95% prediction intervals is approximately ± 25 mg/l TSS. It should be noted that this relationship was established for a range of turbidity between 70 and 660 FAU and was used for turbidities varying between 60 and 700 FAU (average value = 250 FAU).

CALCULATION METHOD

In the case of a discrete sampling of all events for a given year, the pollutant loads M_{pol} for year k could be calculated by sequential summation of loads $M_{j\,pol}$ of all rainfall events (indexed by j with a number N_{events}) that occurred during this year and by sequential summation at time step i (with a number n_j time step), over the duration of each event. It is further assumed that the pollutant load transited during dry weather periods (improper connections, infiltration…) is negligible compared with the one transported during wet weather periods throughout one year. So:

$$M_{pol} = \sum_{j=1}^{N_{events}} M_{pol\,j} \approx \sum_{j=1}^{N_{events}} \sum_{i=1}^{n_j} C_{T-pol\,ji} \times Q_{ji} \times \Delta t_{ji} \quad \text{(Equation 4)}$$

With Q_{ji} = flow rate and $C_{T-pol\,ji}$ = total (i.e. dissolved and particulate) pollutant concentration at time step $i\left(\Delta t_{ji}\right)$ during the event j. The symbol $(\approx)$ indicates that there is a discretization error.

Thus, estimating the mass $M_{j\,pol}$ using the above formula requires knowledge of the dynamics of total pollutant concentration C_{T-pol} and flow rate at each time step. Actually, the details of the dynamics of pollutant loads within a rainfall event is not considered by itself, but only as a mean to get an integrated value of the product $\mathrm{Q_{ji}} \times C_{T-pol\,ji} \times \Delta t_{ji}$ over the

duration of the rainfall event. Thus an analysis performed on a flow-weighted composite sample representative of the entire rainfall event *j* is sufficient for estimating the total pollutant EMC C_{T-pol_j}, and assessing the event load $M_{j\,pol}$ of rainfall event *j* as $M_{j\,pol} = C_{T-pol_j} \times V_j$ (Equation 5) with V_j is the volume of water transported during the rainfall *j*.

Continuous monitoring of flow rate is commonly available, and the equation 5 can be applied to events for which monitoring was carried out for providing C_{T-pol_j}. But pollutant concentrations data are always very scarce, due to sampling and analysis constraints. So we investigate the possible combination of continuous monitoring of some parameters with analyses performed on flow rate averaged event mean samples collected from a few rain events. We especially focus on the added value of turbidity monitoring for improving the assessment of pollutant annual load for pollutants which are significantly correlated with *TSS* EMC.

In this scope, we distinguish two types of pollutants according to the dependence of their total concentrations on TSS concentration. Indeed, the total pollutant concentration C_{T-pol} is expressed as the sum of dissolved $C_{D-pol}(unit/l)$ and particulate $C_{P-pol}(unit/l)$ concentrations (*unit ~ mg* or *µg* or *ng*):

$C_{T-pol} = C_{D-pol} + C_{P-pol} = C_{D-pol} + \tau \times TSS$ (Equation 6), with *TSS(mg/l)* is TSS EMC concentration and τ is the particle pollutant content (*unit/mg TSS*, i.e. τ = particulate concentration / TSS concentration= $C_{P\text{-}pol}/TSS$).

The combination of pollutograph and hydrograph of a rainfall event *j* allows us to estimate the TSS EMC of this rainfall event using (equations 1, 2 and 3).

After identifying the rainfall events in a given year (using precipitation and flow rate time series), from one to four stochastic models are used to handle missing data and finally get an assessment of total pollutant EMC for a given pollutant for any event. Then, an annual flow weighted concentration is derived from the EMC values for all events in one particular year, and the process is repeated by the means of Monte-Carlo simulation to derive a mean value and a confidence interval for each considered pollutant.

Model structures

For a given event, two models are used to handle the lack of continuously monitored data:

1. A precipitation – volume model (model M1) to estimate a value and its uncertainty of the runoff volume of a rainfall event for which there is no flow rate measurement.
2. A TSS EMC model (model M2) to estimate the *TSS* EMC probability distribution of a rainfall event for which neither TSS EMC analysis nor turbidity measurements were available (either due to the lack of sensor or to a drift or failure of available sensors).

In addition, two other models are used to extrapolate data from the few events sampled for pollutant EMC analysis to other events, where such analysis is missing:

3. M3 is used when no correlation between $C_{P\text{-}pol}$ EMC and TSS EMC is identified, and $C_{T\text{-}pol}$ EMC.
4. M4 is used when a significant correlation between $C_{P\text{-}pol}$ EMC and TSS EMC is identified and provides the probability distribution of $C_{T\text{-}pol}$ EMC as the sum of $C_{D\text{-}pol}$

EMC overall probability distribution and $C_{P\text{-}pol}$ EMC probability distribution assessed from TSS EMC value and τ.

M2 and M3 models have no input variable and provide an overall distribution whereas M1 and M4 models use a measured variable (rainfall or TSS) as an input in a linear regression, thus providing a conditional distribution.

Precipitation – volume model (Model M1)

The first model (M1) is a linear model using the runoff coefficient *RC* to estimate the event volume *V* as a function of the precipitation *H* according to the relationship $V = 10 \times A \times RC \times (H - IL)$ where *IL* is the initial loss (in mm) and *A* is the catchment surface area (in ha). For a given catchment, model M1 was fitted by means of least squares method using all the events for which simultaneous flow rate and rainfall intensity are available. *Figure 2* illustrates the runoff model $\left(V = 10 \times A \times RC \times (H\text{-}IL)\right)$ (Equation 7) obtained on each site and the corresponding 95% prediction intervals (95% PI). The obtained runoff coefficients *RC* are reported in *Table 1* above.

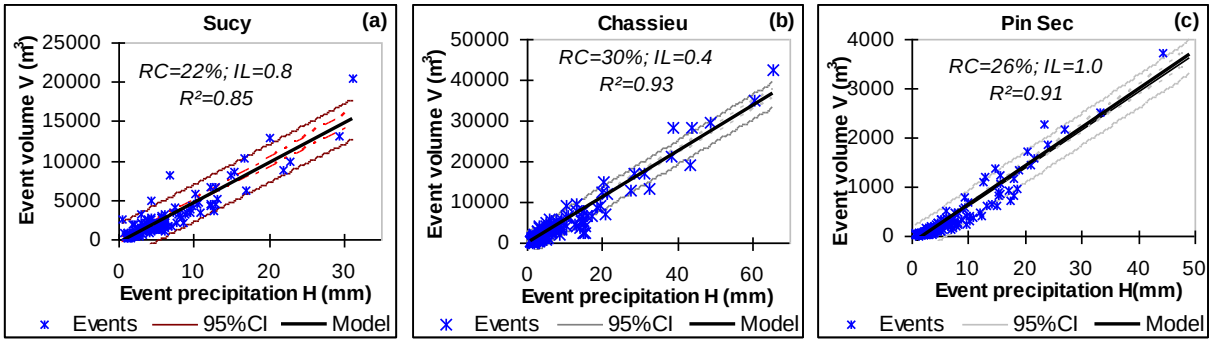

Figure 2: Runoff models and corresponding 95% CI (RC= runoff coefficient, IL = initial loss) for: (a) *Sucy*, (b) *Chassieu* and (c) *Pin Sec*

TSS EMC model (Model M2)

No model could be identified for linking the TSS EMC for a rainfall event to the characteristics of this event (precipitation depth, rainfall intensity, preceding dry weather). A probability distribution model (M2) was used instead and fitted to all TSS measures available on a given site or derived from turbidity measurements. For a given site, the Kolmogorov-Smirnov test was used to fit theoretical and TSS EMC empirical distributions at the 5% level. Different simulations show that the lognormal distribution is well suited for describing the TSS EMC (KS test, α=5%). Hence, both the mean (*m*) and standard deviation (*SD*) of EMCs (estimated distribution) have been calculated first in natural logarithm space (μ and σ mean and standard deviation of $\left(\ln(TSS\ EMC)\right)$ and then transformed into arithmetic space (Romeu 2002) using the formulas: $m = \exp\left(\mu + \sigma^2/2\right)$ and $SD = \sqrt{\exp\left(\sigma^2\right) - 1} \times m$ (Equations 8 & 9) where $\exp(x)$ is the exponential function of *x*. The parameters of fitted distributions for different sites are summarized in *Table 3*.

Table 3: Means and SD of the fitted lognormal distributions of TSS EMC and those of *n* rainfall events on the three sites *Sucy*, *Chassieu* and *Pin Sec*

Site	n	μ	σ	m	SD	KS p-value (1)	$\overline{EMC}$ (2)	σ_{EMC} (2)
Sucy	121	4.83	0.49	141	74	84%	141	73
Chassieu	263	4.63	0.79	140	130	87%	144	144

Pin Sec	18	4.57	0.76	128	114	82%	124	85

(1) p-value for Kolmogorov-Smirnov test; (2) mean and SD calculated on the n rainfall events

Note that the TSS EMCs on both *Sucy* and *Chassieu* sites were calculated from the turbidity data, while those of *Pin Sec* site are those of the measurement campaigns (*Table 6*). Kruskal-Wallis statistical test shows that the distributions of TSS EMCs are not significantly different between the three sites (α = 5% and p-value=17%). In addition, the same test shows that there is no significant difference between the distribution of TSS EMC from one year to another in the same site (*Sucy* and *Chassieu* sites).

$C_{T\text{-}pol}$ EMC models (Models M3 and M4)

As for TSS, no model was identified for assessing the total pollutant EMC $C_{T\text{-}pol}$ according to the characteristics of the corresponding rainfall event. So, a distribution model was applied. *Figure 3* illustrates the methodology of calibration of the distribution model of $C_{T\text{-}pol}$ EMC.

First of all, the significance of the correlation coefficient ($\rho_{TSS\text{-}pol\ part}$) between TSS EMC and particulate concentration $C_{P\text{-}pol}$ EMC was tested for a given pollutant by using Pearson parametric test for normal distribution or Spearman nonparametric test otherwise (α=5% for all these tests). The significance of this correlation leads the choice between two models:

1. No significant correlation: a distribution of $C_{t\text{-}pol}$ EMC (in $\mu g/l$) (model M3) is used. Model distributions are then fitted, using KS test (α=5%) when the number of events is greater than or equal to 6 (Romeu 2003);
2. Significant correlation: a model (model M4) is used, which results from a distribution of contents τ (e.g. $\mu g/mg\ TSS$), a value of *TSS* EMC (e.g. *mg/l*) (obtained by turbidity measurements or M2 model) and a distribution of dissolved concentrations $C_{D\text{-}pol}$ EMC (e.g. $\mu g/l$). The distributions of τ and of $C_{D\text{-}pol}$ EMC are fitted if the number of events is ≥ 6. Then, we calculate the total EMC $C_{t\text{-}pol}$.

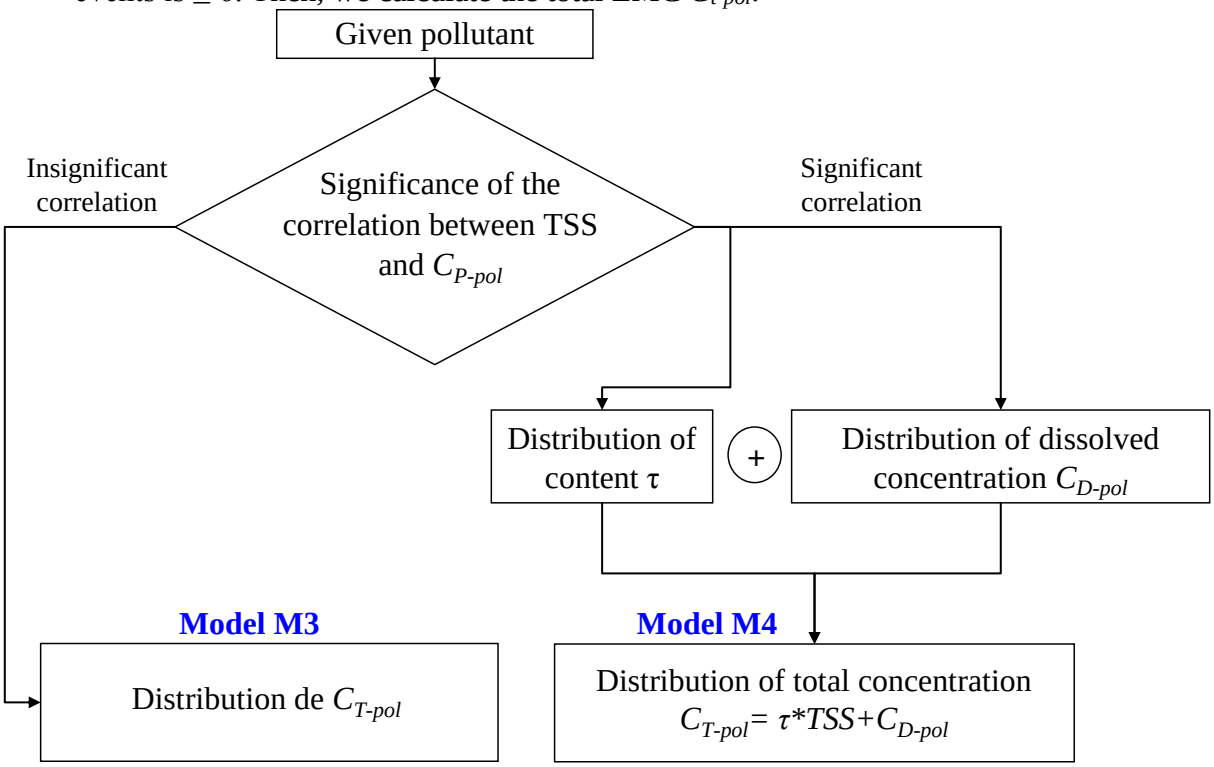

Figure 3: Methodology for deriving the distribution model of EMC for a given pollutant

Furthermore, the rather low number of sampled rainfall events (*Table 1*) is not practical to fit a distribution of EMC for a given pollutant and a given site, especially in the case of *Chassieu* site (2 to 5 measurements per pollutant, *Table 1*). To solve this problem, the data from all three sites were pooled when no significant site-to-site difference between the EMC distributions of this pollutant was detected. Indeed, the homogeneity of $C_{T\text{-}pol}$ EMC for model M3 (or $C_{D\text{-}pol}$ EMC or τ for model M4) for a given pollutant between three sites is verified at the level of 5% (ANOVA parametric test if the homogeneity of variance (Levene's test) and normality (Shapiro-Wilk normality test) are accepted, Kruskal-Wallis non-parametric test otherwise (often used as an alternative to the ANOVA where the assumption of normality is not acceptable)). In the case of rejection of the hypothesis of homogeneity of $C_{T\text{-}pol}$ ($C_{D\text{-}pol}$ EMC or τ), the Siegel–Tukey test of multiple comparisons is applied to find homogeneous groups of sites for a given pollutant. All these statistical tests were performed with the statistical software XLSTAT® (version 2009.3.02, Addinsoft, New York, http://www.xlstat.com).

Kolmogorov-Smirnov test shows that lognormal distributions are well suited to describe pollutants EMCs at the level of 5%: total $C_{T\text{-}pol}$, dissolved $C_{d\text{-}pol}$ and particle contents τ (KS p-value ≥20%). These results are in good agreement with those observed in the literature (EPA 2005, Francey et al. 2010, Mourad et al. 2005, Smullen et al. 1999).
$C_{T\text{-}pol}$ EMC for the different pollutants and groups of pollutants were hence estimated. Indeed, the results for each metal are presented. By contrast, PAHs are presented on the basis of total concentrations, i.e. $\sum_{16} PAH$ (EPA 2005) or $\sum_{13} PAH$ (excluding volatile PAH: N, Acen and Acyl). For PBDE, the results are presented for $\Sigma_{9} PBDE$ and deca-BDE (BDE-209) which displayed the highest concentrations compared to other PBDE. The results of BPA, of octylphenols (∑OP, octylphenol and octylphenol ethoxylates) and nonylphenols (∑NP, nonylphenol and nonylphenol ethoxylates) are also presented.

Figure 4 and ***Erreur ! Source du renvoi introuvable.*** illustrate in the approach applied for two pollutants: ∑OP and Pb. The method presented above is discussed in both figures.
Parameters of the different distributions for models M3 and M4 in natural logarithm space (μ and σ) are reported in *Table 8* in supplementary materials. For more details about the intra and inter-site variability of concentration for a given pollutant, an analysis with a comparison with literature, is detailed in (Gasperi et al. 2014).

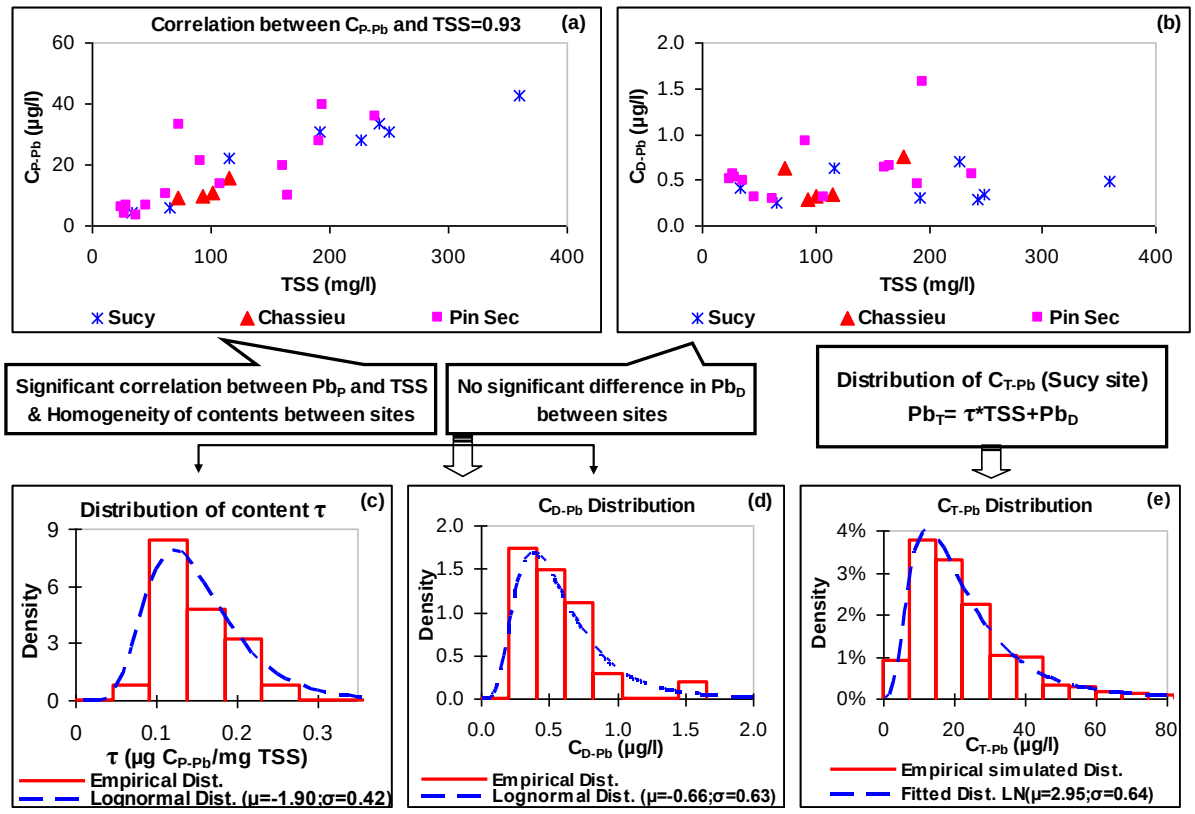

Figure 4: Example of the construction of the model of CT-Pol EMC (M4) for Pb; (e): case of Sucy site

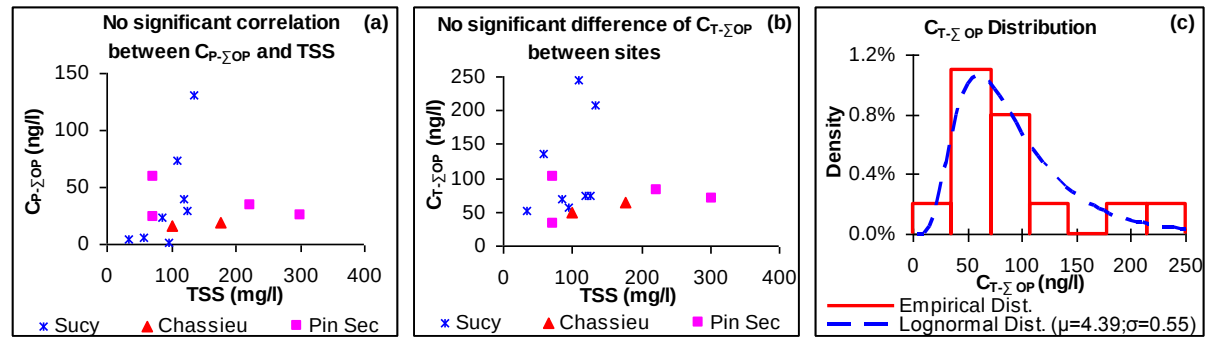

Figure 5: Example of the construction of the model of C_{T-Pol} EMC (M3) for ∑OP

When validated, the lognormal distribution obtained by model M3 is directly used in the calculation of the annual load of this pollutant (example ***Erreur ! Source du renvoi introuvable.*** *c)).*

Alternatively, two independent simulations (condition of independence has been checked using the partition coefficient $K_d = \tau / C_{D-pol}$) using obtained lognormal distributions of τ (*Figure 4 (c)*) and total C_{D-pol} (*Figure 4 (d)*) for a given pollutant are coupled with a TSS concentration (calculated using turbidity or simulated using model M2) to calculate a C_{T-pol} of this pollutant for the corresponding event (*Figure 4 (e)*).

Monte Carlo simulations

Monte Carlo simulations are used to combine the different models detailed above for each particular event in a given year and propagate the probability distributions from each model involved for each event to the annual average values and quantify the associated uncertainties. *Figure 6* illustrates the methodology for assessing pollutant annual load M_{Pol} for a given year and for a given pollutant using a Monte Carlo simulation (ISO/IEC 2008). Note that the

hypothesis of independence between the event volume and concentration was checked for sampled events.

Then, the masses of all the events of this year for a given pollutant are summed up. This process was then reiterated 10,000 times for each year to obtain a probability distribution of annual load M_{Pol}. The average pollutant annual load and the corresponding uncertainties are derived from load distribution by using a 95% confidence interval (shortest 95% confidence interval as recommended by (ISO/IEC 2008) standard).

In addition to sources of variability in the models *M2* to *M4*, various sources of uncertainties are taken into account in the simulation such as:

- Measurement uncertainties: the uncertainties in the measured value are assumed to be normally distributed and independents with their standard uncertainty for:
    - Laboratory analyses: a relative standard deviation (%RSD) equal to 15% (Gromaire and Chebbo 2001, Ruban et al. 2010);
    - Precipitation depth H_j: a %RSD equal to 10%;
    - Flow rate Q_{ij}: a %RSD equal to 10%;
    - Turbidity: a value of 10 FAU or 10 FNU was used as standard uncertainty (Lacour et al. 2009, Metadier and Bertrand-Krajewski 2012).
- Prediction errors of the event volume (Model M1): this one was taken into account using residual errors implied by the linear model established at a given site. Residual errors are homoscedastic and normally distributed;
- Prediction errors of Turbidity-TSS correlation function *f(T)*.

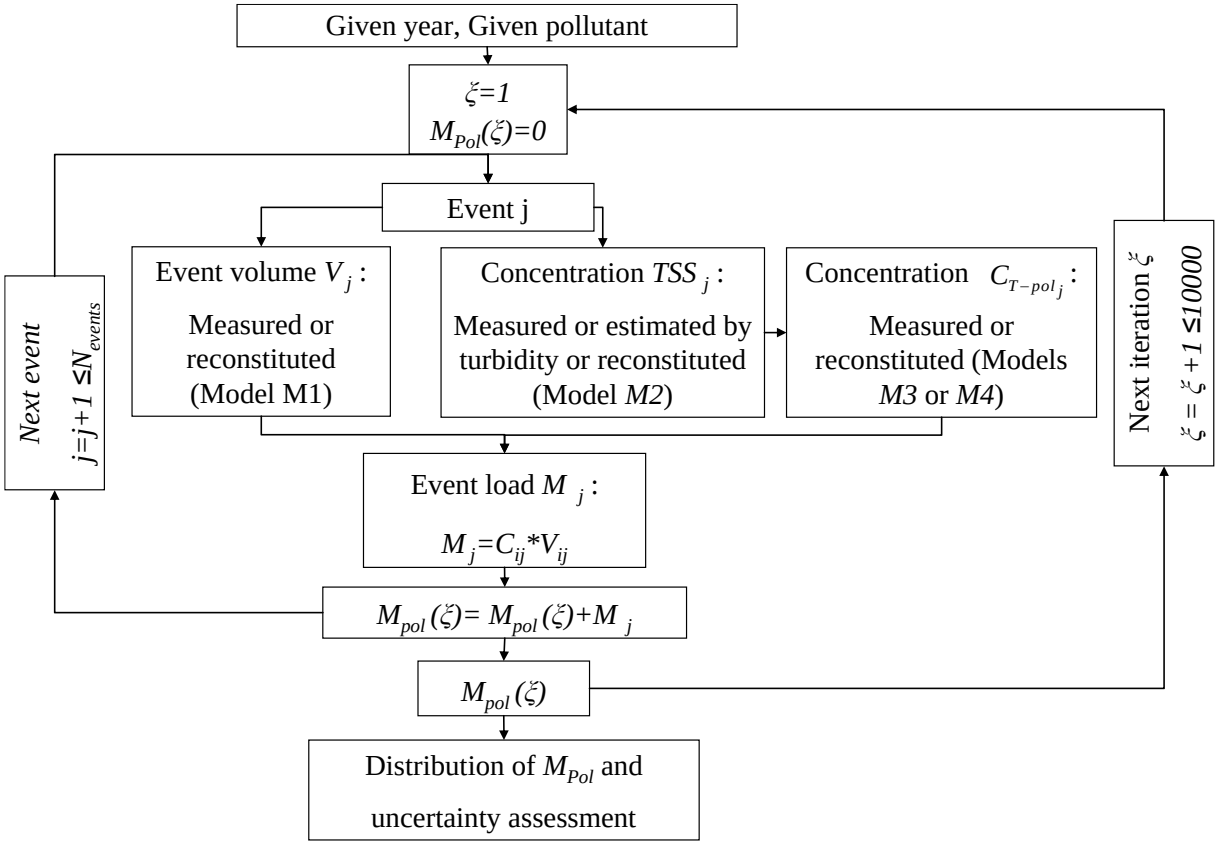

Figure 6: Methodology for assessing pollutant annual loads

The presented methodology has been implemented in Scilab®-5.4.1 open source software (http://www.scilab.org). In the following section, results for TSS and TOC annual loads and those obtained for the different pollutants are discussed. The calculation was performed for 2

years in *Sucy* and *Pin Sec* sites (2011 and 2012) and for 5 years in Chassieu site (2004 to 2008). To compare the results between the three sites, annual loads for each site are normalized by active area (act.ha) and they will be called specific annual loads. The active area S_{act} of a catchment is the area that really contributed to runoff. It was determined by the area *A* of each catchment and the average runoff coefficient *RC* obtained using model M1 (S_{act} = *RC. Area*, see *Table 1* and *Figure 2*). S_{act} is about *50 ha* in Sucy, *55 ha* in Chassieu and *8 ha* in Pin Sec.

APPLICATION ON THE THREE SITES

Annual precipitations and volumes

At the annual scale, the volumes (~net annual precipitation $H_n = (\sum_j H_j\text{-IL})$) expressed in mm (~10 m^3/act.ha) are shown in *Table 4*. The Chassieu site has an annual rainfall greater than that precipitated in *Sucy* and *Pin Sec* sites, which will affect the annual volumes.

Table 4 : Annual volumes on the three studied sites (±95% empirical confidence intervals)

Site	Year	Annual volume Vy/S_{act} (mm = 10 m^3/act.ha)
Sucy	2011	440 ± 10
	2012	525 ± 10
Chassieu	2004	810 ± 15
	2005	580 ± 15
	2006	690 ± 10
	2007	775 ± 10
	2008	840 ± 10
Pin Sec	2011	515 ± 10
	2012	530 ± 10

TSS and TOC annual loads

Specific annual loads of TSS and TOC, for 2 years in *Sucy* and *Pin Sec* sites and for 5 years in *Chassieu* site are illustrated in *Figure 7(a, b)*.

The average values of TSS specific load in *Sucy* and *Pin Sec* sites (between 550 and 700 kg/act.ha/year) are lower than those of the *Chassieu* site (between 700 and 1100 kg/act.ha/year).

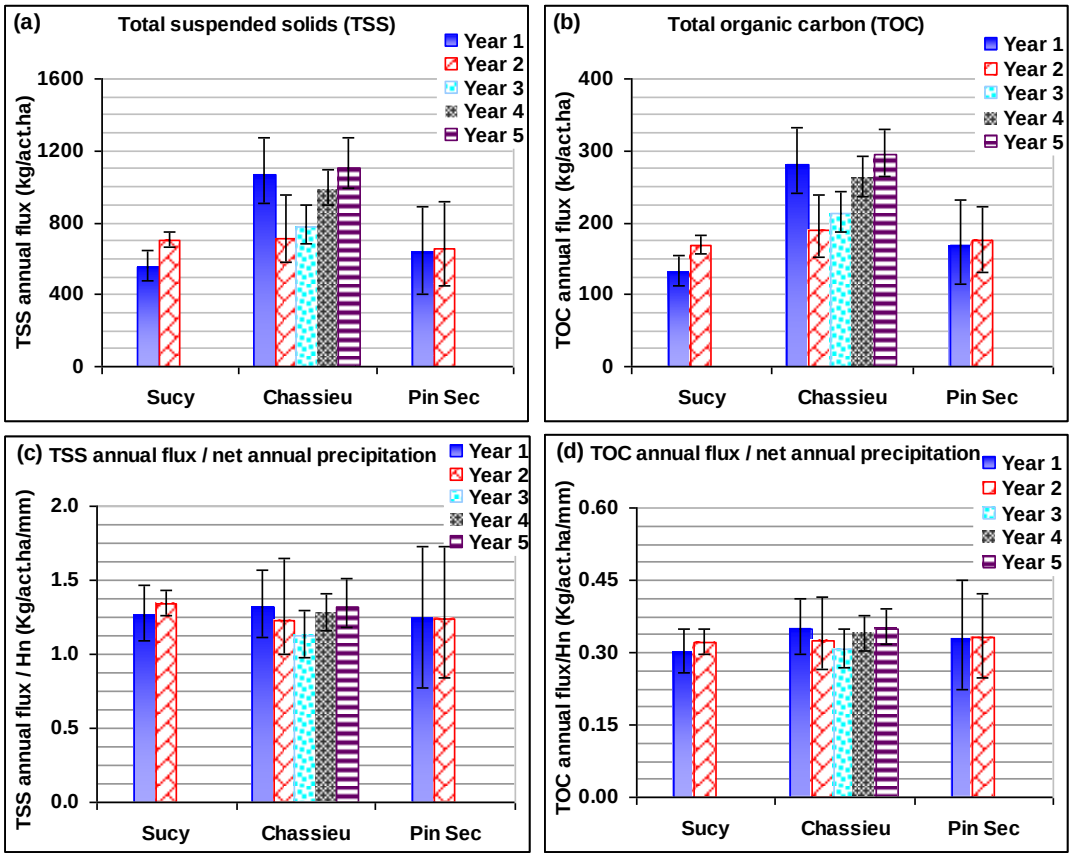

Figure 7: Annual loads at each site (average value from all simulations): (a) TSS annual loads; (b): TOC annual loads; (c) (respectively (d)): TSS (resp. TOC) annual loads per mm of water (net, see *Table 4*). Error bars represent the 95% empirical confidence intervals

Similarly, the same trend can be observed for TOC specific annual loads (between 130 and 175 kg/act.ha/year in *Sucy* and *Pin Sec* and between 190 and 295 kg/act.ha/year in *Chassieu*). At each site, uncertainties on TSS loads and TOC loads vary from one year to another depending on the amount of available data. This dispersion (around the mean value at 95% CI) varies from 5 to 15% in *Sucy* site, from 10 to 35% in *Chassieu* site and from 30 to 40% in *Pin Sec* site. Indeed, two factors affect the uncertainties of TSS loads on the same site: measurement uncertainties and those caused by selected models due to the absence of measurements. The effect of data reconstitution can be spotted on *Sucy* and *Pin Sec*, where fewer data is available in 2011 than in 2012 from flow rate and/or turbidity monitoring and in *Chassieu* where fewer data is available for 2004 and 2005 than for other years due to failures of the measurement system. In addition, the absence of a turbidity measurement in *Pin Sec* site involves uncertainties on the evaluation of annual loads higher than those observed in *Sucy* and *Chassieu* sites.

For temporal variations, we can observe a low inter-annual variability of TSS load with an apparent influence of meteorological conditions expressed as annual precipitation (*Figure 7, (c)*). Indeed, the annual load per mm water (net) represents a Site (discharge–weighted) Mean Concentration (*SMC*). So, the SMC during a given year will be $SMC(mg/l) \cong 10^2 \frac{M(kg/act.ha)}{H_n(mm)}$ (Equation 10). In other words, the overall TSS SMC is about 130±15mg/l in Sucy, 125±45mg/l in Pin Sec and 125±20 mg/l in Chassieu at a confidence level 95%. TSS SMC uncertainty in Pin Sec site is important (~±35%) because it is derived from a small number of rainfall events (n=18). This latter confirms the results of

(Mourad et al. 2005) which stressed that using fewer than 20 sampled rainfall events leads to uncertainties on TSS SMC above 30% (95% half-confidence interval).

Likewise, the overall TOC SMC is about 31±4 mg/l in *Sucy*, 33±10 mg/l in Pin Sec and 33±5 mg/l in *Chassieu* at a 95% confidence level.
Low uncertainties in SS and TOC SMC in Sucy and *Chassieu* sites demonstrates that the use of turbidity monitoring, as indicator of TSS concentration, substantially improves the accuracy of evaluated annual pollutant load.

Annual loads of micropollutants

Annual loads of Pb, $\sum$ OP, $\sum_{16}$ PAH and $\sum_{9}$ PBDE per active hectare are shown in *Figure 8*. The loads are presented for *Sucy* and *Pin Sec* sites. For *Chassieu* the PAH and PBDE loads are not calculated, due to limited number of sampled events. The annual loads of all studied pollutants for all years and their overall SMC are shown in *Table 5*.
We notice an interannual and intersite variability of annual pollutant loads, as for TSS annual loads. At each site, we observe an interannual variability influenced by meteorological conditions (*Table 4*). The inter-site variability of pollutants annual loads per mm water is logically linked to the calibration of distribution models of pollutants EMCs. Indeed, for pollutant displaying site-to-site differences between *Sucy* and *Pin Sec* sites ($\sum_{16}$*PAH* and $\sum_{9}$*PBDE* (see *Figure 7* and *Figure 8* (*c* and *d)*), pollutants annual loads per mm are different between sites. For example, in spite of similar annual precipitation, the $\sum_{16}$*PAH* loads in *Sucy* site are two times higher than those in *Pin Sec* site, but $\sum_{9}$*PBDE* loads in *Sucy* are ten times lower than those in *Pin Sec*, reflecting local contamination.
The Uncertainty on annual loads of different pollutants (at 95% CI) varies between 10 and 60%, and may reach 100% as in the case of $\sum_{9}$*PBDE* in *Pin Sec* site (see *Figure 8* (*d*)). Indeed, we can observe two types of the uncertainties of pollutants loads: i) Loads estimated using model M4: (taking into account the correlation between TSS and pollutant concentration for Zn, Cu, Cr, As, Ni, Pb, Sr, V,$\sum$ NP, $\sum_{16}$PAH (Sucy) and $\sum_{13}$PAH (Sucy)) have dispersion less than 30% around its average values; ii) By comparison those estimated from model M3 (pollutant uncorrelated with TSS like Cd, Co, Pt, Ti, Mo, BDE-209, $\sum_{9}$PBDE, BPA, $\sum$OP, $\sum_{16}$PAH (Pin Sec), $\sum_{13}$PAH (Pin Sec)) have dispersion greater than 30% around its average values and these uncertainties rise to more than 100% in some cases. This shows the importance of a continuous measurement of turbidity minimizing uncertainties in the estimation of annual loads of pollutants attached to solid particles. This point will be illustrated below to show the importance of considering the correlation between TSS and pollutant particulate concentration in the calculation method.

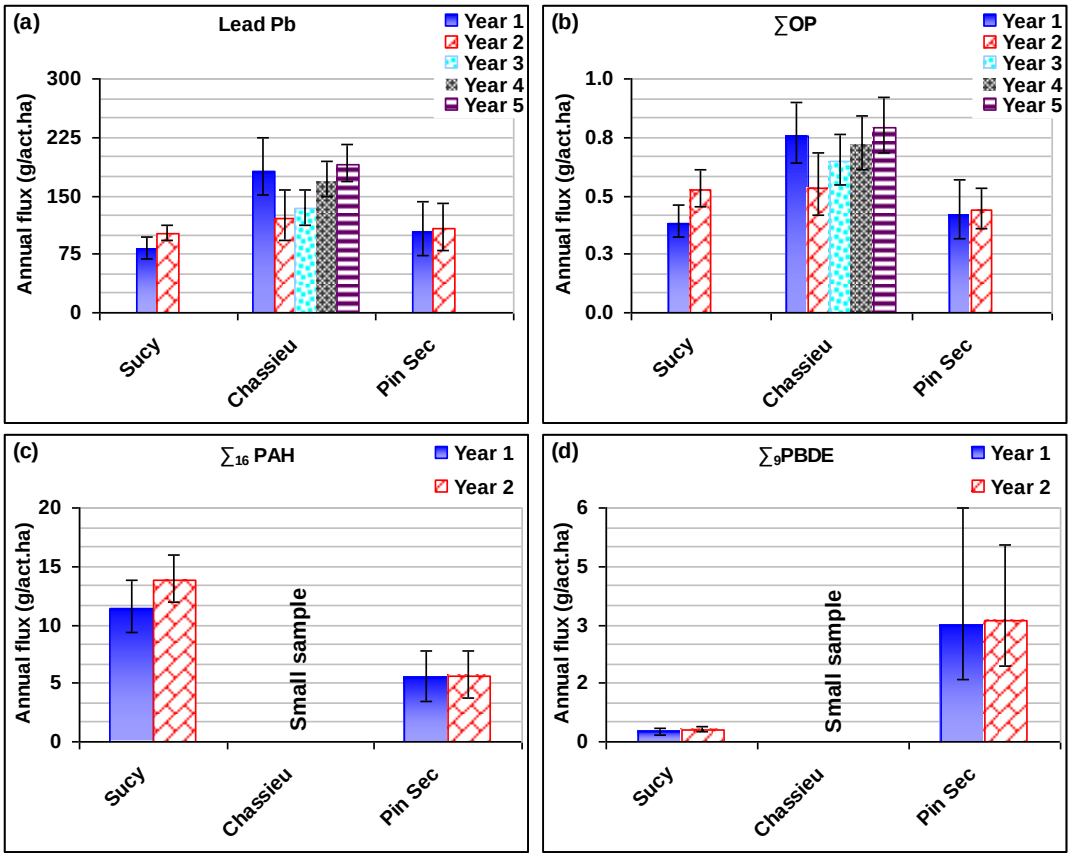

Figure 8: Annual loads at each site of: (a): Lead Pb; (b) sum of Octylphenols ∑OP; (c) sum 16 polycyclic aromatic hydrocarbons ∑16PAH and (d) sum of 9 polybromodiphenylethers ∑9PBDE. Error bars represent the 95% empirical confidence intervals. Years 1 and 2: 2011 and 2012 at Sucy & Pin Sec sites, and Years 1 to 5: 2004 to 2008 at Chassieu site.

Efficiency of turbidity monitoring to reduce uncertainties in annual pollutant loads

To illustrate the impact of correlation ρ between *TSS EMC* and $C_{P\text{-}Pol}$ *EMC*, three cases are simulated and compared for a pollutant having a particulate concentration highly correlated with the concentration of TSS (cases of lead *Pb* for example, see *Figure 4* and *Figure 8*): i) ρ considered as equal to 0 using model M3; ii) ρ considered with its actual value and using model M4 with TSS analyzed on water samples, iii) ρ considered with its actual value using model M4 with TSS assessed from continuous turbidity measurement. The uncertainties involved by the runoff model M1 can be neglected for comparison purpose: uncertainties obtained by this calculation are due only to errors from models M2 (TSS distribution) and M4 (solute distribution plus TSS correlation).

Figure 9 show that this correlation changes the average annual loads as well as its uncertainties. We don't know the "exact value" of *Pb* annual load to validate the average *Pb* annual load obtained for each case. Anyway, the information provided by Pb-TSS correlation lowers the relative uncertainty on the annual concentration, especially if continuous monitoring if turbidity is available. The improvement of the uncertainty observed for case *ii* is explained by the number of events sampled for TSS analysis being larger than the number of events sampled for Pb analysis: 121 rainfall events vs. 24 sampled rainfall events.

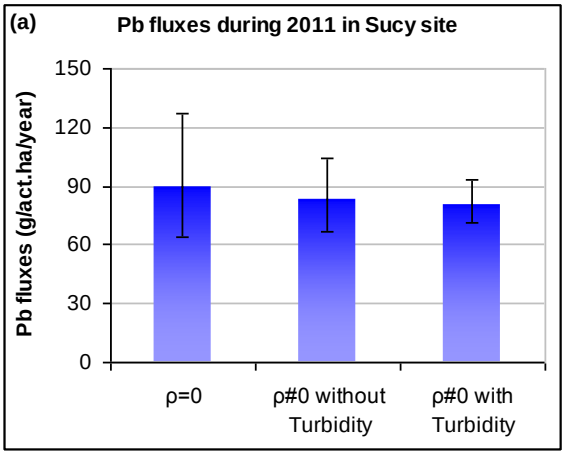

Figure 9: Impact of the correlation between TSS EMC and pollutant particulate EMC with or without turbidity measurements (cases of lead Pb in Sucy site, year 2011)

Table 5: Annual pollutant load per mm water for all years at each site and overall pollutant SMC. Each interval for pollutant load represents the 95% empirical confidence intervals. The intermediate value is the average value of load. * SMC in µg/l. **NE: No evaluated. * SMC in ng/l**

Load (mg/ act.ha/mm)	Poll-utant	As	Cd	Co	Cr	Cu	Mo	Ni	Pb	Pt	Sr	Ti	V	Zn
Sucy	2011	[12;14;15]	[2;2.6;3.4]	[24;31;40]	[26;31;39]	[280;370;490]	[33;48;68]	[37;43;51]	[160;185;220]	[0.34;0.48;0.67]	[920;1085;1285]	[185;245;330]	[38;43;50]	[1530;1800;2120]
	2012	[14;15;16]	[2.3;2.8;3.4]	[28;33;40]	[30;33;36]	[330;380;450]	[40;54;74]	[42;47;53]	[180;195;215]	[0.42;0.54;0.72]	[1070;1220;1400]	[215;255;305]	[43;47;51]	[1760;1920;2110]
	SMC*	**1.4 ± 0.1**	**0.27± 0.04**	**3.2 ± 0.5**	**3.2 ± 0.4**	**38 ± 6**	**5.1 ± 1.4**	**4.5 ± 0.4**	**19 ± 2**	**0.05 ± 0.01**	**116 ± 12**	**25 ± 4**	**4.5 ± 0.4**	**187 ± 16**
Pin Sec	2011	[39;45;53]	[1.9;2.8;4.2]	[23;33;49]	[27;34;44]	[290;410;600]	[26;44;80]	[35;44;57]	[145;205;275]	[0.27;0.45;0.77]	[250;330;430]	[190;270;400]	[38;45;55]	[1590;1920;2360]
	2012	[41;46;51]	[2.2;2.8;3.7]	[26;33;43]	[30;35;41]	[325;413;535]	[31;45;67]	[38;44;53]	[150;200;265]	[0.32;0.45;0.65]	[275;330;395]	[215;270;355]	[40;46;52]	[1710;1940;2220]
	SMC*	**4.6 ± 0.4**	**0.28± 0.06**	**3.3 ± 0.7**	**3.4 ± 0.8**	**41 ± 10**	**4.5 ± 1.7**	**4.4 ± 0.9**	**20 ± 4**	**0.05 ± 0.02**	**33 ± 6**	**27 ± 7**	**4.5 ± 0.5**	**193 ± 28**
Chassieu	2004	[12;15;17]	[2.1;3;3.6]	[26;35;43]	**NE****	[295;440;540]	**NE****	[39;49;57]	[160;225;280]	[0.32;0.51;0.65]	[950;1220;1430]	[195;290;355]	[41;50;57]	[1710;2050;2340]
	2005	[10;14;16]	[1.5;2.8;3.6]	[19;33;42]		[210;410;520]		[32;47;57]	[110;210;270]	[0.23;0.5;0.66]	[770;1150;1400]	[140;270;350]	[34;47;56]	[1400;1940;2310]
	2006	[11;13;15]	[2;2.7;3.2]	[24;31;38]		[275;375;460]		[36;45;52]	[150;190;220]	[0.33;0.51;0.65]	[890;1095;1265]	[180;250;300]	[38;44;50]	[1570;1830;2050]
	2007	[13;14;16]	[2.2;2.9;3.4]	[26;34;41]		[330;425;495]		[38;48;55]	[180;220;240]	[0.33;0.51;0.64]	[975;1185;1360]	[215;280;330]	[43;49;54]	[1760;2000;2200]
	2008	[13;15;16]	[2.3;3;3.5]	[27;36;42]		[340;440;515]		[41;49;56]	[180;225;250]	[0.34;0.52;0.64]	[1020;1225;1400]	[220;290;345]	[44;50;56]	[1820;2070;2280]
	SMC*	**1.4 ± 0.1**	**0.29± 0.03**	**3.4 ± 0.4**		**42 ± 5**		**4.8 ± 0.4**	**21 ± 2**	**0.05 ± 0.01**	**118 ± 10**	**28 ± 3**	**4.84 ± 0.33**	**199 ± 13**

Load (mg/act.ha/mm)	Pollutant	$\sum_{16}$PAH	$\sum_{13}$PAH	BDE-209	$\sum_{9}$PBDE	BPA	∑OP	∑NP
Sucy	2011	[20;26;32]	[20;24;31]	[0.38;0.55;0.8]	[0.41;0.58;0.83]	[3.7;4.6;5.6]	[0.73;0.87;1.05]	[10;12;15]
	2012	[22;26;31]	[22;24;29]	[0.45;0.58;0.74]	[0.48;0.6;0.77]	[4.4;5.2;6.2]	[0.86;1;1.16]	[11;13;15]
	SMC***	**2600 ± 400**	**2400 ± 350**	**57 ± 10**	**59 ± 12**	**490 ± 65**	**95 ± 10**	**1240 ± 150**
Pin Sec	2011	[9;11;13]	[7;9;10]	[0.31;0.58;1.17]	[0.3;0.58;1.21]	[3.1;4.2;6]	[0.61;0.81;1.11]	[9;12;16]
	2012	[9;11;12]	[8;9;10]	[0.37;0.59;0.99]	[0.37;0.59;0.97]	[3.5;4.3;5.4]	[0.68;0.82;1.01]	[10;12;15]
	SMC***	**1060 ± 120**	**875 ± 100**	**58 ± 33**	**58 ± 35**	**430 ± 90**	**80 ± 15**	**1190 ± 250**
Chassieu	2004	**NE****				[4;4.9;5.9]	[0.79;0.93;1.11]	[10;13;15]
	2005					[3.2;4.8;5.8]	[0.65;0.92;1.1]	[8;12;15]
	2006					[3.9;4.9;5.7]	[0.76;0.93;1.07]	[10;12;14]
	2007					[3.8;4.8;5.7]	[0.77;0.93;1.06]	[10;12;14]
	2008					[4;4.9;5.7]	[0.79;0.94;1.08]	[11;13;15]
	SMC***					**490 ± 50**	**95 ± 10**	**1240 ± 110**

CONCLUSIONS

A method was developed to set up annual pollutant loads and its uncertainties using a large dataset of pollutant EMC and continuous turbidity, flow rate and rainfall intensity recordings. This stochastic method is original and allows the coupling between a few event sampling campaigns and continuous measurements of hydrological and water quality parameters (rainfall intensity, flow rate, turbidity).

The results obtained can be summarized as follows:

- Lognormal distributions are well suited to describe pollutant EMC;
- The inter-annual variability of the pollutant annual loads in a given site are mainly influenced by weather conditions (annual precipitation);
- The inter-site variability of the pollutant annual loads per mm of water is related to the distribution of EMC of target pollutant.
- Annual loads of pollutants can be estimated with uncertainties ranging from 10% to 60% and can reach 100% for some pollutants. For the pollutants with a particulate fraction not correlated to TSS concentrations, the dispersion is greater than 30%. For the pollutants highly correlated with TSS concentration, this dispersion can be significantly reduced (10% to 30%) if we have information about TSS concentration (continuous measurement of turbidity).

A continuous measurement of turbidity can improve the estimation of annual loads of some pollutants attached to solid particles. Such results can be used to identify priority sources of pollution and then direct preventive / curative actions.

It would be worthwhile to pursue this line of research at other sites as a preliminary step to generalization.

ACKNOWLEDGMENTS

This study has been conducted within the framework of the INOGEV research program, which was funded by the French National Research Agency (under its "Sustainable Cities" program). The authors would like to thank all project partners, namely the Greater Lyon and RM&C Water Agency, the Nantes Metropolitan Council, the Val-de-Marne Council for their technical and financial support, as well as the French Observatories OPUR, OTHU and ONEVU plus the SOERE URBIS for their scientific contributions. We also highly appreciate the contributions of the authors of papers (Gasperi et al. 2014, Metadier and Bertrand-Krajewski 2012) for collecting and sharing datasets of studied sites.

REFERENCES

2013/39/EU Directive 2013/39/EU of the european parliament and of the council of 12 August 2013: amending Directives 2000/60/EC and 2008/105/EC as regards priority substances in the field of water policy. Official Journal of the European Union, L 226.

Ashley, R., Bertrand-Krajewski, J.L. and Hvitved-Jacobsen, T. (2005) Sewer solids - 20 years of investigation. Water Science and Technology 52(3), 73-84.

Becouze-Lareure, C., Dembélé, A., Coquery, M., Cren-Olivé, C. and Bertrand-Krajewski, J.-L. (2011) Mass balances of priority pollutants from different sources in urban wet weather discharges, p. 8, Porto Alegre/Brazil, 11-16 September 2011.

Clark, S.E., Burian, S., Pitt, R. and Field, R. (2007) Urban wet-weather flows. Water Environment Research 79(10), 1166-1227.

EPA, N. (2005) Alex Maestre and Robert Pitt, The National Stormwater Quality Database, Version 1.1. A Compilation and Analysis of NPDES,Stormwater Monitoring Information. Department of Civil and Environmental Engineering

578 The University of Alabama Tuscaloosa, AL 35294, p. 447.
579 Francey, M., Fletcher, T.D., Deletic, A. and Duncan, H. (2010) New Insights into the Quality
580 of Urban Storm Water in South Eastern Australia. Journal of Environmental Engineering-
581 Asce 136(4).
582 Gasperi, J., Sebastian, C., Ruban, V., Delamain, M., Percot, S., Wiest, L., Mirande, C.,
583 Caupos, E., Demare, D., Md, K., Saad, M., Jj, S., Dubois, P., Fratta, C., Wolff, H., Moilleron,
584 R., Chebbo, G., Cren, C., Millet, M., S, B. and Gromaire, M.C. (2014) "Micropollutants in
585 urban stormwater: occurrence, concentrations, and atmospheric contributions for a wide range
586 of contaminants in three French catchments". Environmental Science and Pollution Research,
587 2014 Apr;21(8):5267-81.
588 Gromaire, M-C., Cabane, P.,Bertrand-Krajewski, J.L., Chebbo, G. (2007). "Utilisation des
589 modèles de calcul des flux polluants en assainissement: résultats d'une enquête en France"
590 (Using pollutant fluxes calculation models in sewer system: results of a survey in France). La
591 Houille Blanche - Revue internationale de l'eau, EDP Sciences, 2007, 2007 (2), pp.94.
592 Gromaire, M.C. and Chebbo, G. (2001) Pollutant concentration measurement uncertainties in
593 sewage. Houille Blanche-Revue Internationale De L Eau (6-7), 109-114.
594 Hannouche, A., Chebbo, G., Ruban, G., Tassin, B., Lemaire, B.J. and Joannis, C. (2011)
595 Relationship between turbidity and total suspended solids concentration within a combined
596 sewer system. Water Science and Technology 64(12), 2445-2452.
597 ISO/IEC (2008) ISO/IEC Guide 98-3/Suppl.1:2008(E) Uncertainty of measurement - Part 3:
598 Guide to the expression of uncertainty in measurement (GUM:1995) Supplement 1:
599 Propagation of distributions using a Monte Carlo method. Geneva (Switzerland): ISO, 2008,
600 98 p.
601 Joannis, C., Ruban, G., Gromaire, M.C., Bertrand-Krajewski, J.L. and Chebbo, G. (2008)
602 Reproducibility and uncertainty of wastewater turbidity measurements. Water Science and
603 Technology 57(10), 1667-1673.
604 Lacour, C., Joannis, C. and Chebbo, G. (2009) Assessment of annual pollutant loads in
605 combined sewers from continuous turbidity measurements: Sensitivity to calibration data.
606 Water Research 43(8), 2179-2190.
607 Langeveld, J.G., Veldkamp, R.G. and Clemens, F. (2005) Suspended solids transport: an
608 analysis based on turbidity measurements and event based fully calibrated hydrodynamic
609 models. Water Science and Technology 52(3), 93-101.
610 Metadier, M. and Bertrand-Krajewski, J.L. (2011) From mess to mass: a methodology for
611 calculating storm event pollutant loads with their uncertainties, from continuous raw data time
612 series. Water Science and Technology 63(3), 369-376.
613 Metadier, M. and Bertrand-Krajewski, J.L. (2012) The use of long-term on-line turbidity
614 measurements for the calculation of urban stormwater pollutant concentrations, loads,
615 pollutographs and intra-event fluxes. Water research 46(20).
616 Mourad, M., Bertrand-Krajewski, J.L. and Chebbo, G. (2005) Sensitivity to experimental data
617 of pollutant site mean concentration in stormwater runoff. Water Science and Technology
618 51(2), 155-162.
619 Mourad, M. and Bertrand-Kralewski, J.L. (2002) A method for automatic validation of long
620 time series of data in urban hydrology. Water Science and Technology 45(4-5), 263-270.
621 Romeu, J.L. (2002) Empirical assessment of normal and lognormal distribution assumptions.
622 RAC START "Reliability Analysis Center, Selected Topics in Assurance Related
623 Technologies". Volume 9, Number 6. Available online
624 (http://src.alionscience.com/pdf/NLDIST.pdf).
625 Romeu, J.L. (2003) Kolmogorov-Simirnov: A Goodness of Fit Test for Small Samples. RAC
626 START "Reliability Analysis Center, Selected Topics in Assurance Related Technologies".
627 Volume 10, Number 6. Available online (https://src.alionscience.com/pdf/K_STest.pdf).

Ruban, G., Mabilais, D. and Lemaire, K. (2010) Particle characterization of urban wet-weather discharges: methods and related uncertainties, p. 10, Graie, Lyon, France.
Sebastian, C., Ruban V., Moilleron R., Barraud S., Chebbo G., Gromaire M-C., Lorgeoux C., Gasperi J., Cren C., Wiest L., Demare D., Millet M., Saad M., Percot S. and D., M. (2011), INOGEV project - an original French approach in micropollutant characterization assessment in urban wet weather effluents and atmospheric deposits. 12nd International Conference on Urban Drainage, Porto Alegre/Brazil, 10-15 September 2011.
Smullen, J.T., Shallcross, A.L. and Cave, K.A. (1999) Updating the US nationwide urban runoff quality data base. Water Science and Technology 39(12), 9-16.
Weiss, P., G. LeFevre and Gulliver, J. (2008) Contamination of Soil and Groundwater Due to Stormwater Infiltration Practices: a Literature Review. University of Minnesota St. Anthony Falls Laboratory Project Report No.515. Prepared for Minnesota Pollution Control Agency. Available June 23, 2008 www.pca.state.mn.us/index.php/download-document.html?gid=7732.
Zgheib, S., Moilleron, R. and Chebbo, G. (2012) Priority pollutants in urban stormwater: Part 1-Case of separate storm sewers. Water Research 46(20), 6683-6692.

SUPPLEMENTARY MATERIALS

Table 6: General characteristics of sampled rainfall events followed by a laboratory analysis in the three studied sites (min-max and median values) (Gasperi et al. 2014)

	H^1 (mm)	Duration (h)	I_{mean} ($mm.h^{-1}$)	I_{max}^2 ($mm.h^{-1}$)	$PDWP^3$ (d)
Sucy (n=24)	1.2-38.6 8.43	0.6-26.3 7.9	0.4-3.8 1.5	2.4-24 7.9	0.17-9.18 2.1
Chassieu (n=7)	2.4-50.0 18.8	3.1-31.6 14.5	0.8-1.7 1.2	4.7-22.7 12.2	0.2-9.8 2.8
Pin Sec (n=18)	2.3-49.9 15.4	2.7-60.5 19.2	0.3-4.0 0.8	2.4-28.8 11.4	0.19-22.29 2.60

1) Precipitation depth; 2) I_{max} evaluated over 5-min intervals; 3) Preceding dry weather period, in days. Min-Max values, as well as median values;

Table 7: Pollutants analyzed and number of rainfall events (Gasperi et al. 2014)

Groups (n=46)	Number of rainfall events	Substances and abbreviations
Metals (n=13)	Sucy: 8 Pin Sec:15 Chassieu: 5	Arsenic (As), Cadmium (Cd), Chromium (Cr), Copper (Cu), Nickel (Ni), Lead (Pb), Zinc (Zn), Platinum (Pt), Vanadium (V), Cobalt (Co), Molybdenum (Mo), Strontium (Sr), Titan (Ti)
PAH (n=16)	Sucy: 8 Pin Sec: 7 Chassieu: 4	Naphthalene (N), Acenaphthylene (Acyl), Acenaphthene (Acen), Fluorene (F), Phenanthrene (P), Anthracene (A), Fluoranthene (Fluo), Pyrene (Pyr), Benzo(a)anthracene (BaA), Chrysene (Chry), Benzo(b)fluoranthene (BbF), Benzo(k)fluoranthene (BkF), Benzo(a)pyrene (BaP), Indeno(cd)pyrene (IP), Dibenzo(ah)anthracene (DahA), Benzo(ghi)perylene (BPer)
PBDE (n=9)	Sucy: 12 Pin Sec: 7 Chassieu: 2	BDE-28 [tri], BDE-47 [tetra], BDE-99 [penta], BDE-100 [penta], BDE-153 [hexa], BDE-154 [hexa], BDE-183 [hepta], BDE-205 [octa], BDE-209 [deca]
Bisphenol A and APnEOs (n=1+7)	Sucy: 12 Pin Sec: 7 Chassieu: 2	Bisphenol A (BPA) Nonylphenol (NP), nonylphenol monoethoxylate (NP1EO), nonylphenol diethoxylate (NP2EO), nonylphenol monocarboxylate (NP1EC), 4-tert-octylphenol (OP), octylphenol monoethoxylate (OP1EO), octylphenol diethoxylate (OP2EO)

Table 8: Parameters of distributions in natural logarithm space (μ and σ) for models M3 ($C_{T\text{-}pol}$) ditribution) and M4 ($C_{D\text{-}pol}$ + τ distributionS). See equations 9 and 10 to switch from the logarithmic space to arithmetic space (m and SD). Note: The units are given in the arithmetic space

Model M3 : $C_{T\text{-}pol}$ (unit)							Model M4: ξ (unit*l/mg TSS) and $C_{d\text{-}pol}$ (unit)							
Substance	*Sucy*		*Chassieu*		*Pin Sec*		Substance	τ and C_d	*Sucy*		*Chassieu*		*Pin Sec*	
	μ	σ	μ	σ	μ	σ			μ	σ	μ	σ	μ	σ
Cd (µg/l)	-1.47	0.81	pooled with Sucy *		as *Sucy*		TOC (mg/l)	τ	1.58	0.21	pooled with Sucy		pooled with Sucy	
								$C_{d\text{-}pol}$	1.53	0.75				
Co (µg/l)	0.95	0.77					Zn (µg/l)	τ	0.42	0.26				
Pt (µg/l)	-3.39	0.92						$C_{d\text{-}pol}$	3.82	0.43				
Ti (µg/l)	2.98	0.84					Cu (µg/l)	τ	-1.28	0.43				
								$C_{d\text{-}pol}$	1.58	0.55				
Mo (µg/l)	1.15	0.98	Small sample: not processed				Cr (µg/l)	τ	-3.52	0.27	Small sample: not processed			
								$C_{d\text{-}pol}$	-1.21	0.52				
$\sum_{16}$ PAH (ng/l)	M3 not relevant: → M4				6.90	0.47	$\sum_{16}$ PAH (ng/l)	τ	3.00	0.52			M4 not relevant → M3	
								$C_{d\text{-}pol}$	5.42	0.63				
$\sum_{13}$ PAH (ng/l)					6.70	0.48	$\sum_{13}$ PAH (ng/l)	τ	3.00	0.51				
								$C_{d\text{-}pol}$	4.81	0.60				
BDE-209 (ng/l)	3.70	0.99			5.47	1.40	As (µg/l)	τ	-4.74	0.20	pooled with Sucy		3.85	0.58
								$C_{d\text{-}pol}$	-0.48	0.17			0.78	0.37
$\sum_{9}$ PBDE (ng/l)	3.64	1.00			5.48	1.39	Ni (µg/l)	τ	-3.49	0.46			pooled with Sucy	
								$C_{d\text{-}pol}$	0.27	0.64				
BPA (ng/l)	6.00	0.62	pooled with Sucy		pooled with Sucy		Pb (µg/l)	τ	-1.90	0.42				
								$C_{d\text{-}pol}$	-0.66	0.63				
							Sr (µg/l)	τ	-1.91	0.43			6.23	0.73
								$C_{d\text{-}pol}$	4.38	0.60			-0.46	0.76
∑ OP (ng/l)	4.39	0.55					V (µg/l)	τ	-3.28	0.33			pooled with Sucy	
								$C_{d\text{-}pol}$	0.31	0.49				
							∑ NP (ng/l)	τ	0.76	0.20				
								$C_{d\text{-}pol}$	6.45	0.65				